Hindawi
Journal of Chemistry
Volume 2017, Article ID 4590952, 10 pages
https://doi.org/10.1155/2017/4590952

*Research Article*

# Modification of Nafion® Membrane via a Sol-Gel Route for Vanadium Redox Flow Energy Storage Battery Applications

**Shu-Ling Huang, Hsin-Fu Yu, and Yung-Sheng Lin**

*Department of Chemical Engineering, National United University, Miaoli 36003, Taiwan*

Correspondence should be addressed to Shu-Ling Huang; simone@nuu.edu.tw and Yung-Sheng Lin; linys@nuu.edu.tw

Received 11 October 2016; Revised 16 December 2016; Accepted 29 December 2016; Published 20 March 2017

Academic Editor: José M. G. Martinho

Copyright © 2017 Shu-Ling Huang et al. This is an open access article distributed under the Creative Commons Attribution License, which permits unrestricted use, distribution, and reproduction in any medium, provided the original work is properly cited.

Nafion 117(N-117)/$SiO_2$-$SO_3H$ modified membranes were prepared using the 3-Mercaptopropyltrimethoxysilane (MPTMS) to react with $H_2O_2$ via in situ sol-gel route. Basic properties including water uptake, contact angle, ion exchange capacity (IEC), vanadium ion permeability, impedance, and conductivity were measured to investigate how they affect the charge-discharge characteristics of a cell. Furthermore, we also set a vanadium redox flow energy battery (VRFB) single cell by the unmodified/modified N-117 membranes as a separated membrane to test its charge/discharge performance and compare the relations among the impedance and efficiency. The results show that the appropriate amount of $SiO_2$-$SO_3H$ led into the N-117 membrane contributive to the improvement of proton conductivity and vanadium ion selectivity. The permeability was effectively decreased from original $3.13 \times 10^{-6}$ $cm^2$/min for unmodified N-117 to $0.13 \times 10^{-6}$ $cm^2$/min for modified membrane. The IEC was raised from original 0.99 mmol/g to 1.24 mmol/g. The modified membrane showed a good cell performance in the VRFB charge/discharge experiment, and the maximum coulombic efficiency was up to 94%, and energy efficiency was 82%. In comparison with unmodified N-117, the energy efficiency of modified membrane had increased more than around 10%.

## 1. Introduction

Search of a higher efficiency, lower pollution, and greener alternative energy has become an important trend for rapid growth of nowadays global economy. Recently, scientists are actively involved in the exploitation of renewable, sustainable, and clean energy, such as wind turbine and photovoltaic, to produce clean and sustainable energy [1, 2]. However, power produced from those devices is fluctuating, and it is easily affected by the climate change. Consequently, electrical energy storage is needed to buffer the peak power on electrical grid. There are several available storage technologies, namely, hydropump, compressed air energy storage, and secondary batteries [3, 4]. Great accomplishment has been made to develop new types of redox flow storage battery (RFB) [5–7]. RFB is a promising energy storage technology due to its low cost and long cycle life, which could be up to 13,000 cycles.

Vanadium redox flow battery (VRFB) is one of the most promising technologies for mid-to-large scale (KW-MW) energy storage, which was first put forward by Sum and Skyllas-Kazacos in 1985 [8]. High cycle life, low cost, reasonable efficiency, and safe operation of VRFB make it very attractive in many energy related applications, such as load leveling, peak shaving, and voltage stabilizing. VRFB is the most mature energy storage technology among others [6, 9, 10]. A constant supply of $V^{2+}/V^{3+}$ ions and $VO^{2+}/VO_2^{+}$ ions, dissolved in sulfuric acid, is provided to the negative and positive electrodes, respectively, through two pumps connected to external storage tanks, as illustrated in Figure 1.

$$VO^{2+} + H_2O \underset{\text{discharge}}{\overset{\text{charge}}{\rightleftharpoons}} VO_2^{+} + 2H^{+} + e^{-} \quad (1)$$

VRFB is a flow battery where electrolytes are circulating between electrolytic cells and storage tank. During charge-discharge cycle, reaction of (4) took place on the electrodes.

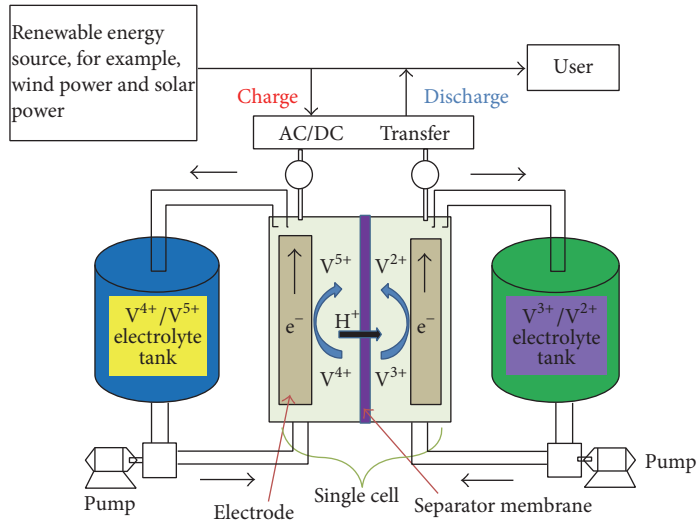


FIGURE 1: Schematic of a vanadium redox flow battery.

Positive half-cell reaction:

$$VO^{2+} + H_2O \underset{\text{discharge}}{\overset{\text{charge}}{\rightleftharpoons}} VO_2^{+} + 2H^+ + e^- \quad (2)$$

Negative half-cell reaction:

$$V^{3+} + e^- \underset{\text{discharge}}{\overset{\text{charge}}{\rightleftharpoons}} V^{2+} \quad (3)$$

Overall reaction:

$$VO^{2+} + V^{3+} + H_2O \underset{\text{discharge}}{\overset{\text{charge}}{\rightleftharpoons}} VO_2^{+} + V^{2+} + 2H^+ \quad (4)$$

The direction of above reactions is reversed, during charge-discharge cycle. Two electrodes are separated by a separation membrane. This membrane is electrical insulated and is highly ionic conductive. The $H^+$ ion is the major charge carrier inside the membrane. However, due to the electrical field and concentration gradient across the membrane, vanadium ions ($VO^{2+}$, $VO_2^{+}$, $V^{+2}$, $V^{+3}$) are also migrated/diffused through the membrane. The crossover of vanadium ions not only reduces the discharge cell voltage but also reduces its Faraday efficiency. During battery operation, the water is transported from one half-cell to the other half-cell by osmosis dragging and diffusion. The phenomena of water transfer cause dilution of one half-cell electrolytes and electrolyte concentration of the other half-cell. The water transport properties of Selemion CMV, AMV, and DMV (Asahi Glass, Japan) had been studied by Mohammadi et al. [11]. Many other composite membranes were also fabricated and tested, including cationic exchange membranes [12–14], anionic exchange membranes [15–17], and amphoteric ion exchange membranes [18, 19]. Nowadays commercial available cationic separate membranes of Nafion based membranes have been developed by DuPont, USA. Although its film has high ionic conductivity, chemical stability, and thermal stability, it cannot overcome the penetration of vanadium ions, which caused the decrease of energy density of battery.

Separation membrane plays an important role in VRFB system. An ideal separated membrane should exhibit low vanadium ions diffusion (crossover) and high proton conductivity. Many modifications were made on Nafion membranes, either to decrease their vanadium permeability or to develop a new membrane with low cost and low vanadium permeability [20–22]. Some investigations [23, 24] have reported that the inorganic-organic hybrid route, sol-gel method, enables inorganic silica or $TiO_2$ particles to be led into the channel structure of Nafion membrane and then improve the cycle performance of the VRFB. In fact, it has been verified that both Nafion/$SiO_2$ and Nafion/$TiO_2$ hybrid membranes show nearly the same IEC and proton conductivity as that of pristine Nafion 117 (N-117) membrane. This could be a promising strategy to overcome the vanadium ions cross-mixed.

Nevertheless, Vijayakumar et al. [25] had proposed explanation with many spectroscopic analyses, showing that $SiO_2$ is still present in the structure of Nafion-$SiO_2$ composite membrane even after 30 cycles of charge/discharge operation, but its ion diffusivity was similar as that of pristine N-117 membrane. Note that under the highly acidic condition porous $SiO_2$ material condenses, shrinks, and forms agglomeration, which in turn decreases the amount of interactions area between $SiO_2$ and Nafion, causing unbinding $V^{4+}$ ion transport via its usual pathway of reversible binding to the sulfonic acid groups of a side of Nafion channel walls.

Based on above deduction, we used the silica bonding sulfonic acid groups ($SiO_2$-$SO_3H$) with the sulfonated 3-mercaptopropyl trimethoxysilane (MPTMS) to react with an oxidized reagent $H_2O_2$ via in situ sol-gel route to modify Nafion membrane, expecting that the unbinding $V^{4+}$ ion can

be bound with either $SiO_2$ or -$SO_3H$ group and avoid binding with the side -$SO_3H$ of Nafion membrane. It could improve the ion crossover and raise the proton conductivity to obtain better cell performances for the VRFB charge/discharge experiment.

## 2. Experimental

*2.1. Materials.* The preparation of N-117/$SiO_2$-$SO_3H$ hybrid membrane was carried out in our laboratory. 3-Mercaptopropyl trimethoxysilane (Acros Organics, USA), peroxide hydrogen ($H_2O_2$) (SHIMAKYU, Japan), vanadyl sulfate ($VOSO_4$) (Alfa Aesar, USA), trimethylamine solution 35% (SHIMAKYU, Japan), $MgSO_4 \cdot 7H_2O$ (SHOWA, Japan), $H_2SO_4$ (Scharlau, Australia), and ethanol, 99.5% (up) anhydrous (ECHO Chemical, Taiwan), were used without further purification. N-117 membranes were purchased from DuPont Inc., USA.

*2.2. The Synthesis of Sulfonated MPTMS.* MPTMS was mixed with EtOH, in MPTMS/EtOH volume ratio of 1 : 5, in a flask equipped with mechanical stirring, followed by adding $H_2O_2$, as an oxidizing agent at room temperature. Under vigorous stirring, a premixed MPTMS/EtOH solution was added into $H_2O_2$ (35 wt%) solution. The volume ratio of MPTMS/EtOH/$H_2O_2$ was ranged from 1 : 5 : 2 to 1 : 5 : 18. In order to understand the oxidative stability of MPTMS, the pH value of the reaction solution was recorded instantaneously under the different $H_2O_2$ adding amount. The thiol group (-SH) and alkoxysilane groups (-$SiOCH_3$) of MPTMS with an oxidizing agent ($H_2O_2$) were oxidized and hydrolyzed to form a sulfonated MPTMS within the Si-OH and $SO_3H$ groups.

*2.3. Preparation of N-117/$SiO_2$-$SO_3H$ Modified Membranes.* The N-117 membranes were pretreated by heating them in a 3% $H_2O_2$ solution at 80°C for one hour, followed by washing with deionized $H_2O$ for 30 minutes at 80°C, then immersed in 1 M $H_2SO_4$ solution for 1 hour at 80°C, and lastly rinsed repeatedly in deionized $H_2O$ to ensure that all membranes were fully protonated before being chemically modified [23, 24]. The pretreated N-117 film was dried for 3 hours at 110°C and then soaked in a sulfonated MPTMS solution (MPTMS/EtOH/$H_2O_2$ = 1 mL : 5 mL : 10 mL) in a two-neck reaction vessel with a mechanical stirrer. The N-117/$SiO_2$-$SO_3H$ membrane was fabricated, and the hydrolysis/polycondensation reaction was allowed to proceed for 0.5 hours (NM-0.5H), 1 hour (NM-1H), and 24 hours (NM-24H), respectively. The formation of $SiO_2$-$SO_3H$ via the sol-gel reaction was embedded to inside channel network of the Nafion membrane.

The structural characteristics of membranes were analyzed using a Fourier transform infrared spectrometer FT-IR (U-2001, HITACHI, Japan) in transmission mode, wavelength ranging from 400 to 4000 $cm^{-1}$, with a 4 $cm^{-1}$ resolution. Thermophysical properties of N-117 and N-117/$SiO_2$-$SO_3H$ hybrid membranes were performed by a differential scanning calorimeter, DSC-Q10 (TA Instruments, USA), in a nitrogen atmosphere, at a heating rate of 10°C/min.

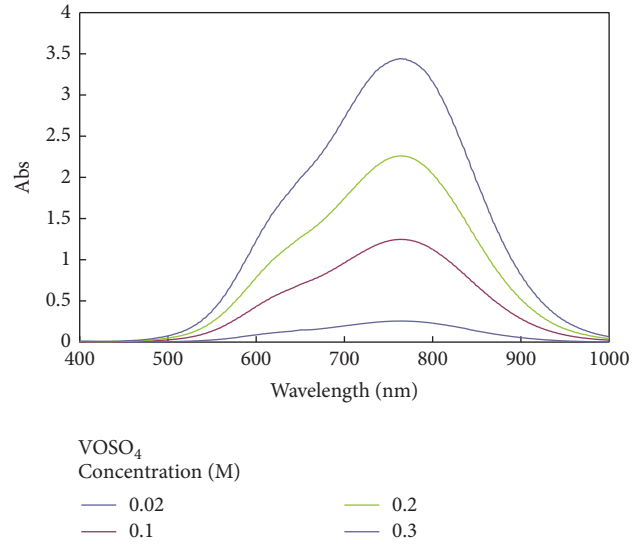


Figure 2: Absorption spectra of $VOSO_4$ solution for four different concentrations at $\lambda_{max}$ = 766 nm.

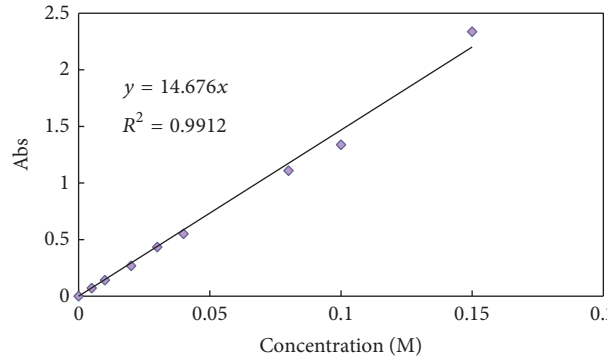


Figure 3: Calibration curve of $VOSO_4$ solution with the concentration range between 0.005 M and 0.15 M.

*2.4. Membrane Properties*

*2.4.1. Vanadium Ion Permeability.* The rate change of the vanadium ion in $VOSO_4$ solution absorbance is used to calculate the diffusion coefficient, that is, permeability, according to Fick's First Law and Beer's Law [26]. The diffusion cell has two compartments, compartment A and compartment B. The former was filled with 50 mL of 2.0 M $VOSO_4$/2.0 M $H_2SO_4$ solution, and the latter was filled with 50 mL of 2.0 M $MgSO_4$/2.0 M $H_2SO_4$ solution.

Figure 2 is the spectra of $VOSO_4$ solution at four different concentrations, and the maximum absorption peak for $VO^{2+}$ ions is located at 766 nm. A calibration curve based on the results of Figure 2 was carried out in the concentration range from 0.005 to 0.15 M $VOSO_4$ solution, at wavelength $\lambda_{max}$ = 766 nm, as shown in Figure 3.

*2.4.2. Water Uptake and Contact Angle.* The water uptake is defined as the ratio of the weight of absorbed water to that of the dry membrane. The water uptake was calculated by (5).

$$\text{Water uptake} = \frac{W_W - W_d}{W_d} \times 100\%, \quad (5)$$

where $W_W$ is the weight of the wetted membrane after the membrane is immersed in $H_2O$ for 24 hours and $W_d$ is the weight of the dry membrane. The contact angle between the water and the membranes was directly measured by a contact angle measuring instrument (FTA-125, APPR, Germany) for evaluation of their hydrophilic/hydrophobic properties.

*2.4.3. Ion Exchange Capacity.* Ion exchange capacity was measured by the typical acid-base titration (inverse-titrated method). Membranes in acidic form were first immersed in excessive 0.1 M NaOH solution for 24 hours to exchange the fixed $H^+$ ions by $Na^+$ ions. The unreacted NaOH solution with membrane was inverse-titrated by 0.1 M HCl solution, and the IEC could be calculated by (6):

$$\text{IEC} = \frac{N_{\text{NaOH}} V_{\text{NaOH}} - N_{\text{HCl}} V_{\text{HCl}}}{W_{\text{sample}}}, \quad (6)$$

where $N_{\text{NaOH}} \times V_{\text{NaOH}}$ is the total mmoles of NaOH and $N_{\text{HCl}} \times V_{\text{HCl}}$ is consumed moles by HCl solution inverse-titrated.

*2.4.4. Resistance and Ionic Conductivity.* The membrane ionic conductivity was measured with a single cell. The membrane was sandwiched between two composite graphite plates. Flow channels on the carbon plate were filled with 2.0 M $VOSO_4$/2.0 M $H_2SO_4$ solution. The electrochemical impedance spectroscopy (EIS) of this single cell with different membranes was measured with a Frequency Response Detector & Potentiostats system (Princeton Applied Research, FRD100&VersaSTAT™, USA). The sinusoidal excitation voltage applied to the cells was 10 mV with a frequency range between 0.1 Hz and 100 kHz. Proton conductivity ($\kappa$) and area resistance were calculated by (7) and (8).

$$\kappa = \frac{L}{R \times A}, \quad (7)$$

$$R_A = (R_1 - R_2) \times A, \quad (8)$$

where $A$ is area, $L$ is thickness, $R$ is electric resistance, $\kappa$ is conductivity, and $R_1$ and $R_2$ are the electric resistance of the cell with and without a membrane, respectively.

*2.5. Single Cell Performance of VRFB.* An H-type single cell for charge-discharge experiments was designed by Green Energy and Environmental Lab. of Industrial Technology Research Institute, Taiwan. The single cell of VRFB is consisted of two pieces of carbon paper (Shenhe Carbon Fiber Materials Co., Ltd.) and two current collectors. The VRFB for charge-discharge test was performed by sandwiching the membrane between two pieces of graphite carbon paper electrodes. A 2.0 M $VOSO_4$/2.0 M $H_2SO_4$ solution was employed as negative and positive electrolytes. The effective area of electrode was 5 × 5 $cm^2$ and the volume of the electrolytes solution in each half-cell was 30 mL and cyclically pumped into the corresponding half-cell. The charge and discharge test was carried out using a Battery Cycler Test System (WBCS3000S, WonATech, Korea) and CT2001C-10 V/2 A (Wuhan Land Co., China) between 0.8 and 1.8 V at a current density of 20 mA $cm^{-2}$.

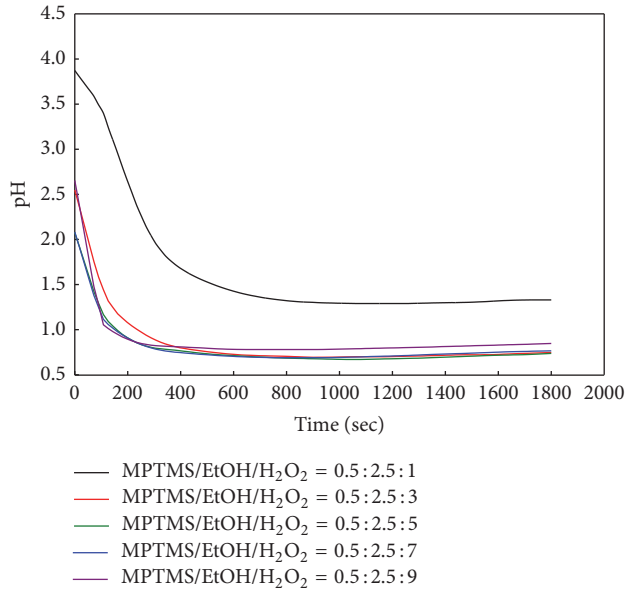


Figure 4: The reaction time dependence of pH value for the sulfonated MPTMS solution.

## 3. Results

*3.1. Preparation of N-117/$SiO_2$-$SO_3H$ Hybrid Membranes*

*3.1.1. The Syntheses of Sulfonated MPTMS and N-117/$SiO_2$-$SO_3H$ Hybrid Membranes.* MPTMS was oxidized by an oxidizing agent, $H_2O_2$ in EtOH solution to form a strong sulfuric acid (-$SO_3H$) group. The pH value of the sulfonated solution was reduced with increase of reaction time. Figure 4 shows that the pH of the solution decreases strongly for all $H_2O_2$ contents in the first 400 s. The more complete the sulfonated reaction of MPTMS, the lower the pH value it reaches. This is due to the formation of sulfonic acid groups. The solution has the lowest pH value at a MPTMS/EtOH/$H_2O_2$ volume ratio of 0.5 : 2.5 : 5.

The N-117/$SiO_2$-$SO_3H$ hybrid membranes were prepared using the sulfonated MPTMS to react with an oxidized reagent $H_2O_2$ via sol-gel method. The content of $SiO_2$-$SO_3H$ increases with the increasing of sol-gel reaction time, as shown in Table 1. The $SiO_2$-$SO_3H$ content of samples NM-0.5H, NM-1H, and NM-24H was 1.51 wt%, 1.91 wt%, and 1.99 wt%, respectively.

*3.1.2. FT-IR Spectra of Membranes.* The structural comparison of N-117/$SiO_2$-$SO_3H$ and pretreated N-117 membranes

Table 1: Comparison of basic properties of N-117 and N-117/$SiO_2$-$SO_3H$ membranes.

| Samples | $SiO_2$-$SO_3H$ (wt%) | Thickness ($\mu$m) | Contact angle Angle (°) | Water uptake (wt%) | IEC (mmol/g) | Permeability ($\times 10^{-6}$ $cm^2$/min) |
|---|---|---|---|---|---|---|
| N-117 | 0.00 | 195 ± 5 | 86 ± 2 | 21 | 0.99 | 3.13 |
| NM-0.5H | 1.51 | 195 ± 5 | 86 ± 2 | 17 | 1.23 | 0.20 |
| NM-1H | 1.91 | 195 ± 5 | 86 ± 2 | 17 | 1.24 | 0.13 |
| NM-24H | 1.99 | 195 ± 5 | 86 ± 2 | 18 | 1.24 | 0.12 |

The reaction times for NM-0.5H, NM-1H, and NM-24H were 0.5 h, 1 h, and 24 h, respectively.

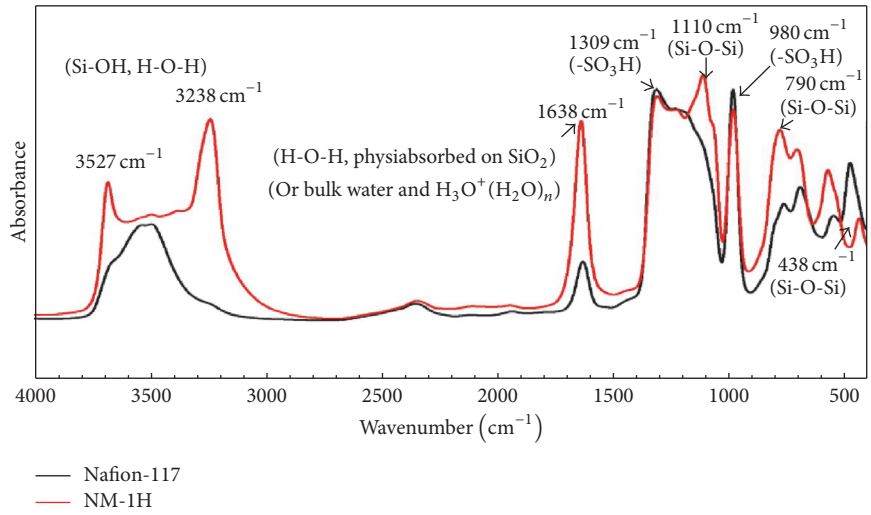


Figure 5: FT-IR spectra and for the pretreated N-117 and NM-1H modified membranes.

was confirmed by FT-IR spectra, as shown in Figure 5. The spectrum of the N-117 membrane has been reported in previous research [27]. In comparing spectrum of N-117 with NM-1H, a new peak at 1110 $cm^{-1}$ can be observed, which is attributed to the vibration of Si-O-Si groups [24, 28, 29]. However, there are not any new peaks of N-117 membrane found in that region. In addition, Figure 5 (red line) shows there is one specific peak appearing at 3238 $cm^{-1}$. This peak is corresponding to the O-H stretching vibration of $SO_3H$ groups [28, 29].

Furthermore, for both spectrums of N-117 and NM-1H, the band at 1309 $cm^{-1}$ is from the antisymmetric $CF_3$ stretch, which appears overlapped with the antisymmetric and symmetric $CF_2$ stretching modes, around 1230 and 1150 $cm^{-1}$, and S=O antisymmetric and symmetric stretching bands from $SO_3H$ groups would appear at 1435 and 1320 $cm^{-1}$, respectively [24]. There are no peaks found in 2500~2600 $cm^{-1}$ (stretching vibration of -SH group) for the NM-1H, which indicates the -SH groups of MPTS have been oxidized to sulfonic acid groups [27]. Moreover, there is a stronger absorption peak at 1638 $cm^{-1}$ for NM-1H membrane, showing that some physical-absorbed water may be present in the NM-1H membrane. That is associated with $SiO_2$ particles and either bulk water, $(H_2O)_n$, or highly hydrated oxonium ions, $H_3O^+(H_2O)_n$ [25, 27].

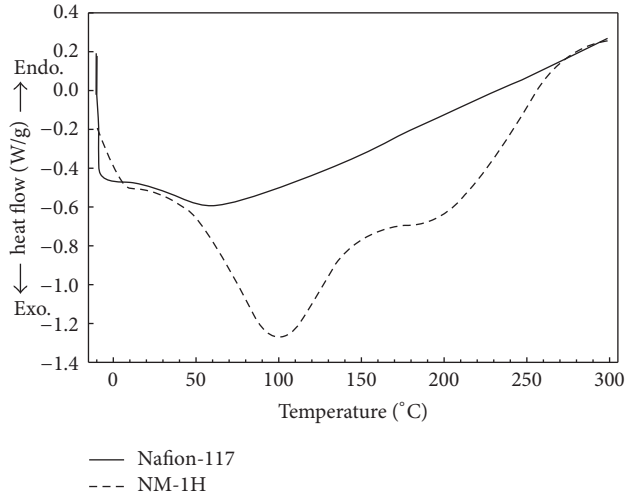


Figure 6: DSC thermogram of N-117and NM-1H modified membranes, in a nitrogen atmosphere at a heating rate of 10°C/min.

*3.1.3. DSC.* The DSC thermograms (Figure 6) also imply the formation of the Si-O-Si groups. The exothermic peaks appear at 100°C and around 178°C corresponding to the release of $H_2O$ molecules and formation of the Si-O-Si

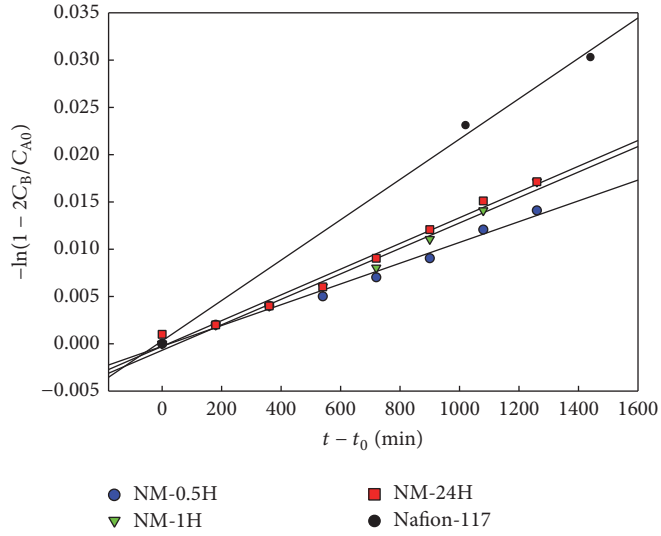


Figure 7: The vanadium concentration is plotted as a function of time according to (9).

groups which come from the condensation of Si-OH [30] and formation of crystalline $SiO_2$ particles and release of $H_2O$ for sample NM-1H. The unmodified N-117 has not shown any peaks in these regions.

### 3.2. Basic Properties of Membranes

*3.2.1. Vanadium Ion ($V^{4+}$) Permeability.* The membrane was placed between two compartments, compartment A and compartment B, and vanadium concentration in compartment B ($C_B$) was measured after experimental time $t$ from the calibration curve in Figure 3.

According to the previous literature [31], $V^{4+}$ permeability can be obtained by (9). $t_0$ is the initial time of experiment, and $t_0$ is equal to zero in this case. $C_{A0}$ is the initial vanadium concentration and $P$ is permeability. $A$ and $L$ are the membrane area and thickness, respectively. $V_B$ is the solution volume in compartment B.

$$-\ln\left(1-\frac{2C_B(t)}{C_{A0}}\right)=\frac{PA}{V_BL}(t-t_0). \quad (9)$$

The logarithmic function of vanadium concentration is calculated according to (9) and is plotted as a function of time in Figure 7. As shown in Figure 7, a linear behavior of $-\ln[1-(2C_B/C_{A0})]$ versus $(t-t_0)$ was obtained. The permeability was calculated from the slope of Figure 7, and detailed data were summarized on Table 1. As exhibited in Figure 7 and Table 1, the permeability of membranes N-117/$SiO_2$-$SO_3H$, NM-0.5H, NM-1H, and NM-24H is $3.13\times10^{-6}$ cm$^2$/min, $0.2\times10^{-6}$ cm$^2$/min, $0.13\times10^{-6}$ cm$^2$/min, and $0.12\times10^{-6}$ cm$^2$/min, respectively.

*3.2.2. Water Uptake, Contact Angle, IEC, and Other Properties of Membranes.* Table 1 lists basic properties of four membranes, N-117, NM-0.5H, NM-1H, and NM-24H, including water uptake, contact angle, IEC, and permeability. Water uptake is one of basic factors of ion exchange membrane. An optimal amount of water uptake enables the membrane to achieve good ion conductivity. The membrane contains excessive water uptake which results in the vanadium ion cross-over mixing and even reduces its mechanical properties. The water uptakes of the modified N-117 membranes (NM-0.5H, NM-1H, and NM-24H) are in the range of 17 to 18 wt%, which are lower than that of N-117 which is 21 wt%.

Contact angles were measured to evaluate the changes in the hydrophilic/hydrophobic properties. In general case, Nafion series membranes are water-swellable. When water droplets come into contact with membrane, the membrane was swollen by water, and a projection phenomenon could be observed on the surface of membrane as exhibited in Figure 8. The contact angles of the N-117/$SiO_2$-$SO_3H$ membranes were in the range of $82\pm2^\circ$ to $86\pm2^\circ$, which are slightly lower than that of N-117($88^\circ\pm2$). These hybrid membranes were slightly hydrophilic.

IEC is defined as the ability of $H^+$ proton to exchange between positive and negative electrolytes. The separate membrane with a high IEC will exhibit great proton conductivity for VRFB system. As listed in Table 1, the IEC for an unmodified N-117 and three modified membranes, NM-0.5H, NM-1H, and NM-24H, are 0.99 mmol/g, 1.23 mmol/g, 1.24 mmol/g, and 1.24 mmol/g, respectively. The ion exchange capacity increases with the reaction time and $SiO_2$-$SO_3H$ from NM-0.5H to NM-1H. There is no further increase when the reaction time is extended to 24 hours. It can be found that the modified membranes have improved its IEC by using the sulfonated MPTMS.

*3.3. Electrochemical Impedance Spectroscopy.* The membrane conductivity was measured with a single cell. A cationic exchange membrane (N-117) was used as both separator and reference for comparison with the modified membranes. The resistance, area resistance, and conductivity of membranes can be estimated from the electrochemical impedance spectroscopy data. The Nyquist plots and Equivalent circuit are

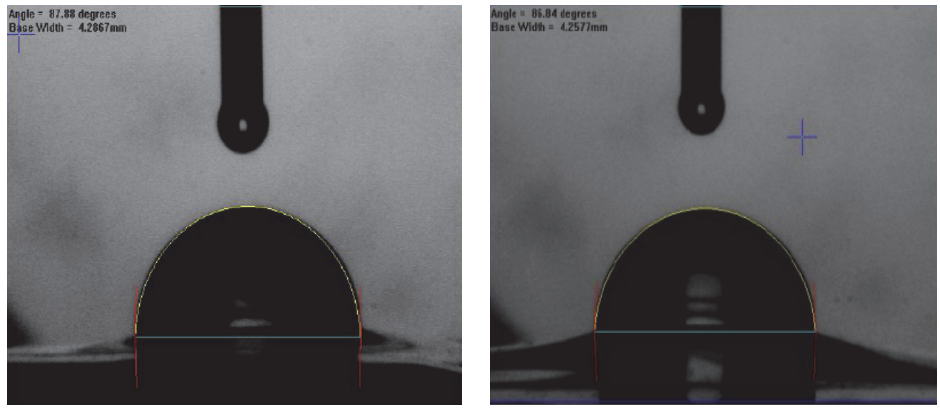


(a) Three seconds (b) 30 seconds

Figure 8: Water drops into the NM-1H membrane; after 30 secs, the membrane was swollen and caused a projection phenomenon.

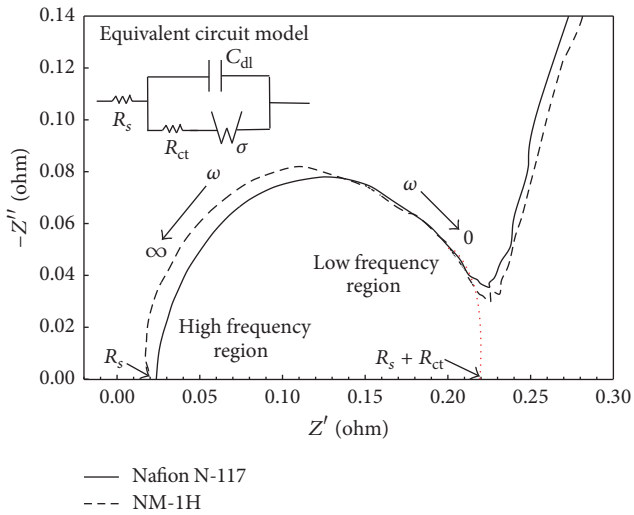


Figure 9: Nyquist plots of the impedance data for N-117 and NM-1H membranes.

often used to model the electrochemical system. Figure 9 is the Nyquist plots of the impedance data with the simulating Equivalent circuit model for N-117 and NM-1H sample.

The semicircle in high frequency region is concerned with the charge transfer process. The membrane resistance $R_s$ representing the resistance of electrolyte solution can be obtained from the intercept of the impedance curve on the $x$-axis at frequency close to infinity, that is, at $Z''$ = 0. The charge transfer resistance $R_s + R_{ct}$ is related to across electrode/solution interface charge transfer process. The semicircle $R_{ct}$ is the charge transfer resistance of the electrode, as similar to $R_s$, and can be obtained from the semicircle diameter at frequency close to zero and at $Z''$ = 0 [32, 33].

The semicircle in low frequency region represents the mass diffusion control process. This resistance is called Warburg resistance when the electrochemical system achieves in mass transfer control process. The Warburg resistance equals $2 \times C_{dl}\sigma^2 - R_s - R_{ct}$, where $C_{dl}$ is electric double layer capacity and $\sigma$ is Warburg constant. The resistance ($R_s$ and $R_A$) and conductivity of N-117 and modified membranes were summarized in Table 2.

Table 2: Comparison of resistance and conductivity for N-117 as well as modified membranes.

| Samples | $R_S$ (mΩ) | Area resistance ($R_A$) (Ω×cm$^2$) | Conductivity (mS/cm) |
|---|---|---|---|
| Nafion N-117 | 23.70 | 0.59 | 33.05 |
| NM-1H | 22.32 | 0.56 | 34.82 |
| NM-24H | 36.40 | 0.91 | 21.43 |

The $R_s$ value of membranes is in the order as NM-24H (36.40 mΩ), N-117 (23.70 m Ω), NM-1H (22.32 mΩ). The NM-1H modified membrane has a slightly lower area resistance ($R_A$ = 0.56 Ωcm$^2$) than that of N-117 ($R_A$ = 0.59 Ωcm$^2$). In general, a membrane with high area resistance exhibits low conductivity.

*3.4. Single Cell Performance for VRFB System.* A single cell for VRFB was charged to 1.8 V and discharged to 0.8 V at a constant current density of 20 mA/cm$^2$. The columbic efficiency (CE), voltage efficiency (VE), and energy efficiency (EE) are defined according to (10):

$$\begin{aligned} \text{CE} &= \frac{C_{\text{discharge}}}{C_{\text{charge}}} \times 100\%, \\ \text{VE} &= \frac{V_{\text{discharge}}}{V_{\text{charge}}} \times 100\%, \\ \text{EE} &= \text{CE} \times \text{VE}, \end{aligned} \tag{10}$$

where $C_{\text{charge}}$ and $C_{\text{discharge}}$ are charge/discharge capacity and $V_{\text{charge}}$ and $V_{\text{discharge}}$ are the middle point voltage of charge/discharge, respectively. The higher CE, meaning lower capacity loss, is mainly due to the lower crossover diffusion rate for vanadium ions and the side reactions. Higher VE

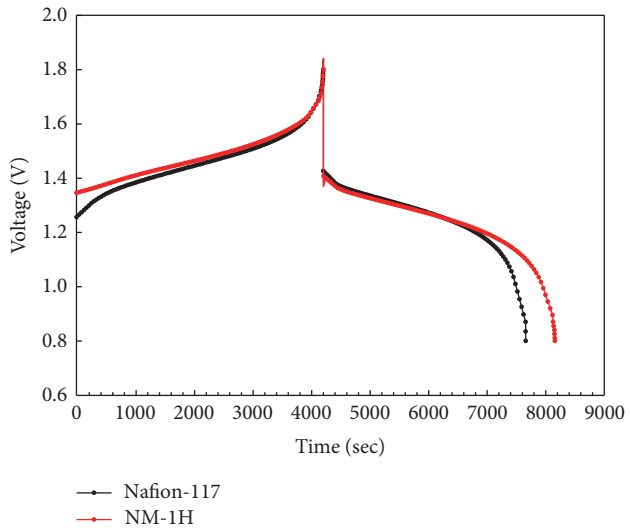


Figure 10: Charge-discharge curves of single cell performance for VRFB by N-117 and NM-1H membrane, respectively, as a separator; a current density is 20 mA $cm^{-2}$.

Table 3: The single cell efficiency for VRFB system based on the pristine N-117 membrane and modified NM-1H membrane.

| Samples | Coulombic efficiency (%) | Voltage efficiency (%) | Energy efficiency (%) |
|---|---|---|---|
| N-117 | 82 | 87 | 71 |
| NM-1H | 94 | 87 | 82 |

indicates lower battery resistances, which are referred to the electrodes, separator, flow path, and so on.

The charge-discharge experiments were carried out by a single cell. Figure 10 displays the charge-discharge curves of the VRFB with a 2.0 M vanadium electrolyte and using N-117 and NM-1H modified membrane as a separator, respectively. Comparing the charge-discharge curves of VRFB between N-117 and NM-1H modified membranes, we can find that the discharge capacity of the VRFB with NM-1H modified membrane is higher than N-117 membrane. The relationships among the CE, VE, and EE are listed in Table 3. The CE and EE of the VRFB with NM-1H membrane are 94% and 82%, and the CE and EE of the VRFB for N-117 membrane are 82% and 71%, respectively. The VE of the VRFB is close to around 87% for both N-117 and NM-1H membrane. The VRFB with NM-1H modified membrane displays higher CE and EE than that of N-117 membrane.

## 4. Discussion

The investigation of the pH change for sulfonated MPTMS solution and the FTIR spectra in Figures 4 and 5 shows that the present condition of synthesis, at a MPTMS/EtOH/$H_2O_2$ volume ratio of 1 : 5 : 10, enables the MPTMS to be oxidized completely.

By full hydrolysis/polycondensation and in situ sol-gel route, the inorganic $SiO_2$-$SO_3H$ groups are introduced into the channel network structure of N-117 membrane. The deposition of $SiO_2$ particle on the N-117 membrane can be confirmed by the presence of a new absorption band and a specific band, at 1110 $cm^{-1}$ and 1638 $cm^{-1}$ of the FTIR spectra, which are referred to Si-O-Si groups and physiabsorbed water associated with $SiO_2$ particles.

Furthermore, the stretching vibration absorption peak of -SH group in the MPTST disappeared in the range of 2500~2600 $cm^{-1}$, and the specific surfonic acid bands in the range 900~1000 $cm^{-1}$ and 1300~1400 $cm^{-1}$ can be observed for the NM-1H modified membrane. It can be corroborated that the -SH groups of MPTS have been oxidized to the sulfonic acid groups. Summarizing these FT-IR spectra and DSC data, it can be established that the N-117/$SiO_2$-$SO_3H$ modified membranes could be successfully synthesized via the sol-gel reaction.

By combining the results from the basic properties of membranes in Table 1, the contact angle of NM-1H membrane, 86° ± 2, is similar to that of N-117, 88° ± 2. This can be explained as follows: the strong hydrophilicity of sulfonated group can reduce the contact angle, but the hydrophobicity of silica group will cause the contact angles to increase, under the cross effect between the hydrophilic and hydrophobic groups; the contact angles of hybrid membranes are similar to that of N-117. The water uptake of the hybrid membranes is based on above reasons, too.

In addition, Table 1 shows that the permeability of modified membrane reduces obviously with the reaction time, and the $SiO_2$-$SO_3H$ amounts are increased with reaction time. However, the formation of $SiO_2$-$SO_3H$ via the sol-gel route grafting on the channel network of the Nafion membrane reaches equilibrium after reacting around one hour; hence the permeability of NM-1H sample, $0.13 \times 10^{-6}$ $cm^2$/min, is similar to that of NM-24H sample, $0.12 \times 10^{-6}$ $cm^2$/min. It is clear that the permeability was effectively decreased for modified membrane, because $SiO_2$-$SO_3H$ particles result in the polar clusters inside the Nafion membrane and hinder the vanadium ion diffusion. In fact, these results verified that both Nafion/$SiO_2$ and Nafion/$TiO_2$ hybrid membrane show nearly the same IEC and proton conductivity as that of pristine N-117 membrane. The results of this research suggest that this approach is a promising strategy to overcome the vanadium ions cross-mixed problem.

From Table 1, it can be proved that the IEC of N-117/$SiO_2$-$SO_3H$ modified membrane was raised more, and the permeability was reduced stronger than those of other references [23–25]. The outcomes can be attributed to the introduction of silica and surfonic acid groups into the pore cluster of N-117.

In the same case, resistance and conductivity data of N-117/$SiO_2$-$SO_3H$ modified membrane for the EIS test of VRFB shown in Table 2 indicate the proton conductivity of NM-1H modified membrane is higher than that of N-117, signifying that the increasing proton conductivity is referred to the $SiO_2$-$SO_3H$ immobilized in the network channel of N-117. At the same time, the NH-24H modified membrane

has the lowest proton conductivity. As shown in Table 1, the IEC of NH-24H membrane is the same as that of NM-1H membrane, implying that the equivalent of sulfonic acid for both NH-1H and NH-24H is equal. However, the $SiO_2$-$SO_3H$ amount of NH-24H membrane, 1.99 wt%, is larger than that of NM-1H, 1.91 wt%, inferring that the $SiO_2$ content of NH-24H is more than that of NM-1H, but its -$SO_3H$ groups are similar to that of NM-1H. It can be deduced that the higher resistance for NH-24H sample was ascribed to the $SiO_2$ particles.

Furthermore, as shown in Figure 10 and Table 3, test data of a vanadium redox single cell performance, it can be seen that the columbic efficiency of the single cell using NM-1H as a separator was increased from 82% to 94%; fortunately, the voltage efficiency was not reduced, holding at 87%. Related references [23–25] revealed that the voltage efficiency of modified membrane was reduced because of the higher area resistance of $SiO_2$ or $TiO_2$ inorganic particles.

The EE of the NM-1H modified membrane is higher than that of unmodified N-117. It could be attributed to the -$SO_3H$ groups of NM-1H membrane having improved the proton conductivity and the $SiO_2$-$SO_3H$ groups having restrained vanadium ion cross-mixed, especially shown in the increase of CE.

## 5. Conclusions

The present condition of synthesis, at a MPTMS/EtOH/$H_2O_2$ volume ratio of 1 : 5 : 10, enables the MPTMS to be oxidized completely to form a sulfonated $SiO_2$-$SO_3H$ functional group. The N-117/$SiO_2$-$SO_3H$ modified membranes could be synthesized using an oxidation reaction and a simple sol-gel route. It can be confirmed by FT-IR spectra and DSC that the $SiO_2$-$SO_3H$ groups can be successfully grafted on the N-117 network structure to form modified membranes. The permeability was effectively decreased and the ion exchange capacity was raised obviously for modified membrane. It is mainly attributed to its $SiO_2$-$SO_3H$ particles which hinder the diffusion of vanadium ion and then improve the transfer of $H^+$ proton.

In the EIS test of VRFB, the improvement of proton conductivity can be attributed to the introduction of $SiO_2$-$SO_3H$ into the Nafion channel network; however, excessive $SiO_2$ in the modified membrane would cause the resistance to increase. The NM-1H modified membrane has a lower $R_s$, lower area resistance, and higher proton conductivity than those of unmodified N-117 membrane. Hence, the NM-1H sample exhibits a superior cell performance than the pristine N-117 in the VRFB charge/discharge experiment. The maximum coulombic efficiency is up to 94%, and energy efficiency is 82% for the NM-1H modified membrane.

## Competing Interests

The authors declare that there is no conflict of interests regarding the publication of this paper.

## Acknowledgments

This work was supported by the Ministry of Science and Technology, Taiwan, under Grant no. MOST 105-2221-E-239-031.

## References

[1] H. Lund and B. V. Mathiesen, "Energy system analysis of 100% renewable energy systems—the case of Denmark in years 2030 and 2050," *Energy*, vol. 34, no. 5, pp. 524–531, 2009.

[2] S. Vazquez, S. M. Lukic, E. Galvan, L. G. Franquelo, and J. M. Carrasco, "Energy storage systems for transport and grid applications," *IEEE Transactions on Industrial Electronics*, vol. 57, no. 12, pp. 3881–3895, 2010.

[3] H. Lund and G. Salgi, "The role of compressed air energy storage (CAES) in future sustainable energy systems," *Energy Conversion and Management*, vol. 50, no. 5, pp. 1172–1179, 2009.

[4] Á. J. Duque, E. D. Castronuovo, I. Sánchez, and J. Usaola, "Optimal operation of a pumped-storage hydro plant that compensates the imbalances of a wind power producer," *Electric Power Systems Research*, vol. 81, no. 9, pp. 1767–1777, 2011.

[5] S. Ha and K. G. Gallagher, "Estimating the system price of redox flow batteries for grid storage," *Journal of Power Sources*, vol. 296, pp. 122–132, 2015.

[6] A. Lucas and S. Chondrogiannis, "Smart grid energy storage controller for frequency regulation and peak shaving, using a vanadium redox flow battery," *International Journal of Electrical Power & Energy Systems*, vol. 80, pp. 26–36, 2016.

[7] Y. Zeng, T. Zhao, X. Zhou, L. Wei, and H. Jiang, "A low-cost iron-cadmium redox flow battery for large-scale energy storage," *Journal of Power Sources*, vol. 330, pp. 55–60, 2016.

[8] E. Sum and M. Skyllas-Kazacos, "A study of the V(II)/V(III) redox couple for redox flow cell applications," *Journal of Power Sources*, vol. 15, no. 2-3, pp. 179–190, 1985.

[9] C. Fabjan, J. Garche, B. Harrer et al., "The vanadium redox-battery: an efficient storage unit for photovoltaic systems," *Electrochimica Acta*, vol. 47, no. 5, pp. 825–831, 2001.

[10] C. J. Rydh and B. A. Sandén, "Energy analysis of batteries in photovoltaic systems. Part I: performance and energy requirements," *Energy Conversion and Management*, vol. 46, no. 11-12, pp. 1957–1979, 2005.

[11] T. Mohammadi, S. C. Chieng, and M. S. Kazacos, "Water transport study across commercial ion exchange membranes in the vanadium redox flow battery," *Journal of Membrane Science*, vol. 133, no. 2, pp. 151–159, 1997.

[12] T. Mohammadi and M. Skyllas-Kazacos, "Preparation of sulfonated composite membrane for vanadium redox flow battery applications," *Journal of Membrane Science*, vol. 107, no. 1-2, pp. 35–45, 1995.

[13] W. Wei, H. Zhang, X. Li, Z. Mai, and H. Zhang, "Poly(tetrafluoroethylene) reinforced sulfonated poly(ether ether ketone) membranes for vanadium redox flow battery application," *Journal of Power Sources*, vol. 208, pp. 421–425, 2012.

[14] J. G. Austing, C. N. Kirchner, L. Komsiyska, and G. Wittstock, "Layer-by-layer modification of Nafion membranes for increased life-time and efficiency of vanadium/air redox flow batteries," *Journal of Membrane Science*, vol. 510, pp. 259–269, 2016.

[15] T. Mohammadi and M. Skyllas Kazacos, "Modification of anion-exchange membranes for vanadium redox flow battery

applications," *Journal of Power Sources*, vol. 63, no. 2, pp. 179–186, 1996.

[16] B. Zhang, S. Zhang, D. Xing, R. Han, C. Yin, and X. Jian, "Quaternized poly(phthalazinone ether ketone ketone) anion exchange membrane with low permeability of vanadium ions for vanadium redox flow battery application," *Journal of Power Sources*, vol. 217, pp. 296–302, 2012.

[17] L. Zeng, T. Zhao, L. Wei, Y. Zeng, and Z. Zhang, "Highly stable pyridinium-functionalized cross-linked anion exchange membranes for all vanadium redox flow batteries," *Journal of Power Sources*, vol. 331, pp. 452–461, 2016.

[18] G. Hu, Y. Wang, J. Ma et al., "A novel amphoteric ion exchange membrane synthesized by radiation-induced grafting $\alpha$-methylstyrene and N,N-dimethylaminoethyl methacrylate for vanadium redox flow battery application," *Journal of Membrane Science*, vol. 407-408, pp. 184–192, 2012.

[19] J. B. Liao, M. Z. Lu, Y. Q. Chu, and J. L. Wang, "Ultra-low vanadium ion diffusion amphoteric ion-exchange membranes for all-vanadium redox flow batteries," *Journal of Power Sources*, vol. 282, pp. 241–247, 2015.

[20] Q. Luo, H. Zhang, J. Chen, D. You, C. Sun, and Y. Zhang, "Preparation and characterization of Nafion/SPEEK layered composite membrane and its application in vanadium redox flow battery," *Journal of Membrane Science*, vol. 325, no. 2, pp. 553–558, 2008.

[21] J. Zeng, C. Jiang, Y. Wang et al., "Studies on polypyrrole modified nafion membrane for vanadium redox flow battery," *Electrochemistry Communications*, vol. 10, no. 3, pp. 372–375, 2008.

[22] B. Schwenzer, S. Kim, M. Vijayakumar, Z. Yang, and J. Liu, "Correlation of structural differences between Nafion/polyaniline and Nafion/polypyrrole composite membranes and observed transport properties," *Journal of Membrane Science*, vol. 372, no. 1-2, pp. 11–19, 2011.

[23] J. Xi, Z. Wu, X. Qiu, and L. Chen, "Nafion/$SiO_2$ hybrid membrane for vanadium redox flow battery," *Journal of Power Sources*, vol. 166, no. 2, pp. 531–536, 2007.

[24] X. Teng, Y. Zhao, J. Xi, Z. Wu, X. Qiu, and L. Chen, "Nafion/organic silica modified $TiO_2$ composite membrane for vanadium redox flow battery via in situ sol-gel reactions," *Journal of Membrane Science*, vol. 341, no. 1-2, pp. 149–154, 2009.

[25] M. Vijayakumar, B. Schwenzer, S. Kim et al., "Investigation of local environments in Nafion$SiO_2$ composite membranes used in vanadium redox flow batteries," *Solid State Nuclear Magnetic Resonance*, vol. 42, pp. 71–80, 2012.

[26] X. Teng, Y. Zhao, J. Xi, Z. Wu, X. Qiu, and L. Chen, "Nafion/organic silica modified $TiO_2$ composite membrane for vanadium redox flow battery via in situ sol-gel reactions," *Journal of Membrane Science*, vol. 341, pp. 149–154, 2009.

[27] D. Chen, S. Wang, M. Xiao, D. Han, and Y. Meng, "Sulfonated poly (fluorenyl ether ketone) membrane with embedded silica rich layer and enhanced proton selectivity for vanadium redox flow battery," *Journal of Power Sources*, vol. 195, no. 22, pp. 7701–7708, 2010.

[28] A. Fidalgo and L. M. Ilharco, "The defect structure of sol–gel-derived silica/polytetrahydrofuran hybrid films by FTIR," *Journal of Non-Crystalline Solids*, vol. 283, no. 1-3, pp. 144–154, 2001.

[29] S. K. Young, W. L. Jarrett, and K. A. Mauritz, "Nafion®/ORMOSIL nanocomposites via polymer-in situ sol–gel reactions. 1. Probe of ORMOSIL phase nanostructures by $^{29}Si$ solid-state NMR spectroscopy," *Polymer*, vol. 43, no. 8, pp. 2311–2320, 2002.

[30] F. Rubio, J. Rubio, and J. L. Oteo, "A DSC study of the drying process of TEOS derived wet silica gels," *Thermochimica Acta*, vol. 307, no. 1, pp. 51–56, 1997.

[31] M. Bello, "Assessment of electrochemical methods for methanol crossover measurement through PEM of direct methanol fuel cell," *International Journal of Engineering & Technology*, vol. 11, pp. 92–111, 2011.

[32] M. Sluyters-Rehbach and J. H. Sluyters, *Comprehensive Treatise of Electrochemistry*, vol. 9, Plenum, New York, NY, USA, 1984.

[33] M. S. Rehbach and J. H. Sluyters, *Electroanalytical Chemistry*, vol. 4, Marcel Dekker, New York, NY, USA, 1970.

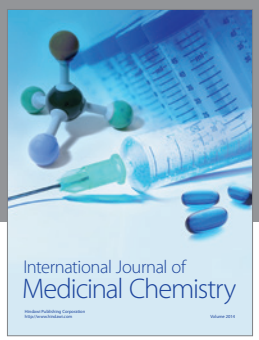

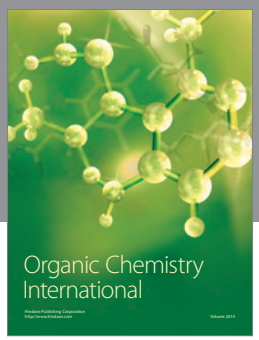

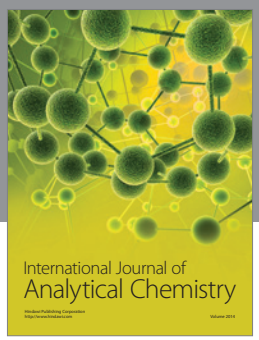

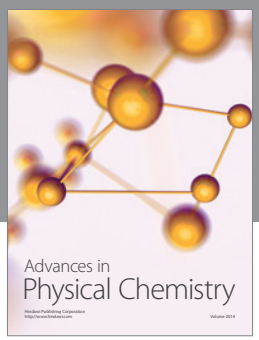

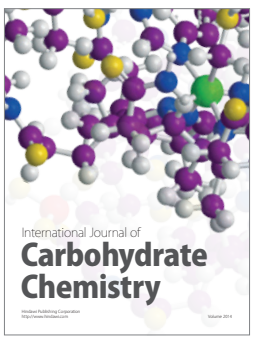

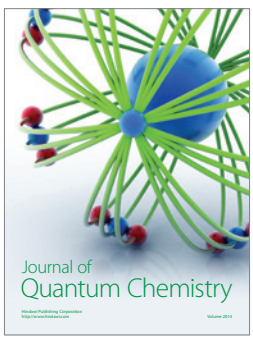

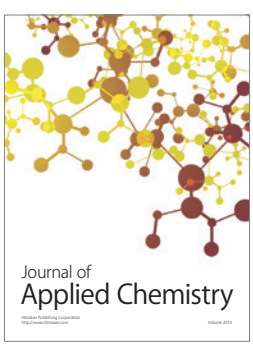

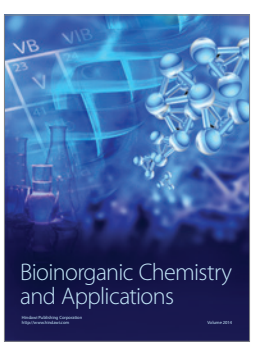

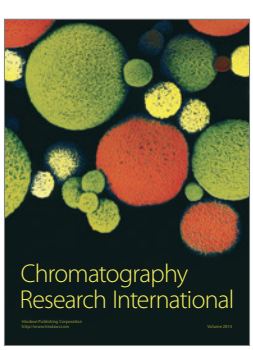

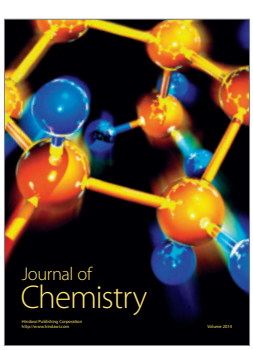


Hindawi

Submit your manuscripts at
https://www.hindawi.com